Plasma Rotation Braking and Driving in Tokamaks

L.-J. Zheng 1), M. T. Kotschenreuther 1), J. W. Van Dam 1), F. L. Waelbroeck 1), M. S. Chu 2)

1) Institute for Fusion Studies, The University of Texas at Austin, Austin, Texas 78712, USA
2) General Atomics, P.O. Box 85608, San Diego, California 92186, USA

e-mail contact of main author: lzheng@mail.utexas.edu

Abstract. Plasma rotation is important for tokamak confinement because it can stabilize MHD modes (such as the resistive wall mode) and help reduce anomalous transport. In this work we address several issues related to plasma rotation in tokamaks: (1) We show that the resonance for static error-field amplification in tokamak plasmas occurs at the no-wall stability limit, rather than at the resistive wall mode stability limit predicted earlier; this new result is consistent with experimental observations. We calculate the error field-induced torque in ITER. (2) We find that a liquid metal wall can shield the effect of an error field by eliminating resonant amplification and reversing the self-enhancing nature of rotation braking. (3) We propose an explanation for spontaneous rotation generation observed during ion and electron cyclotron heating, based on acceleration of trapped minority tail particles via their toroidal precessional drift, and find good comparison of the theoretical predictions with key experimental features.

1. Resonant Error Field Amplification and Rotation Braking

Recent DIII-D experiments showed that rotation spins down even in the presence of continuous, unbalanced neutral beam injection [1], indicating the existence of a strong braking torque. Static error-field-induced torque was proposed by Boozer [2] as an explanation for rotation braking and investigated experimentally [3].

However, there is some confusion related to this explanation. For one thing, the expression for the torque in Refs. [2, 5] contains parameters whose relationship to the no-wall and conducting-wall potential energies is not explicitly determined. It was concluded that the resonance of static error field amplification (*i.e.*, the maximum for the induced torque) occurs at the resistive wall mode stability limit (when the amplification phase is 90 degrees). Experiments were carried out on DIII-D in order to check this picture. Garofalo *et al.* [6] developed a method for empirically determining the static error-field-induced torque profile and also concluded that the torque maximum occurs at the resistive wall mode stability limit, but this conclusion was based on an overly simplified theoretical model. In fact, as Gimblett and Hastie [4] pointed out, the prediction in Ref. [2] that the resonance for static error-field amplification occurs at the resistive wall mode stability limit is inconsistent with the direct experimental measurements [1], which show that rotation spin-down precedes the no-wall stability limit, rather than the resistive wall mode stability limit.

In our work we have derived a new expression for the error-field-induced torque, with all the parameters explicitly defined. With our explicit torque expression, we find that the resonance of the static-error-field amplification in tokamak plasmas occurs at the no-wall stability limit. Our theoretical prediction solves the concern raised in Ref. [4] about the conformity with experimental observation of the rotation braking mechanism based on static error-field-induced torque. Our theory indicates that the rotation braking occurs at a much lower beta than the RWM stability limit for a rotating plasma, which is consistent with the experimental observations in Ref. [1].

Technically, our approach is two-fold: First, we used the jump in the tangential magnetic field to specify the error-field strength, since the error field current is directly related to this jump through Ampere's Law. Conventional treatments use the normal magnetic

field to specify the error-field strength, but this introduces complexity since the normal magnetic field is continuous across the thin error-field current layer. Second, instead of calculating the torque on the plasma, we calculate the torque on the wall and the error-field current layer, which is opposite in direction but equal in magnitude to the torque on the plasma that causes braking of plasma rotation. Our new, completely explicit expression clearly shows that the torque maximum occurs at the no-wall stability limit and not at the resistive wall stability limit.

We briefly describe the derivation procedure; details are given in Ref. [7]. We use a thin-wall approximation to model the error-field current layer. We assume, without loss of generality, that the error-field current layer is located immediately outside the resistive wall. Hence we consider a system in which the plasma torus is surrounded by an inner vacuum region; the inner vacuum region is enclosed by a thin resistive wall; immediately outside the resistive wall is a thin error-field current layer; and outside the error-field current layer is an outer vacuum region extending to infinity. The toroidally axisymmetric equilibrium magnetic field is expressed as $\vec{B} = \boldsymbol{\nabla}\phi \times \boldsymbol{\nabla}\psi + g(\psi)\boldsymbol{\nabla}\phi$, where ψ is the radial flux coordinate, θ is the poloidal angle, and ϕ is the toroidal angle. Since the error field is small compared to the equilibrium magnetic field, linear perturbation theory can be used to evaluate its effect. Then, by matching the independent solutions in the plasma and inner and outer vacuum regions across the plasma-vacuum interface and the resistive wall, we derive the following resistive wall mode equation that includes the effect of an error field:

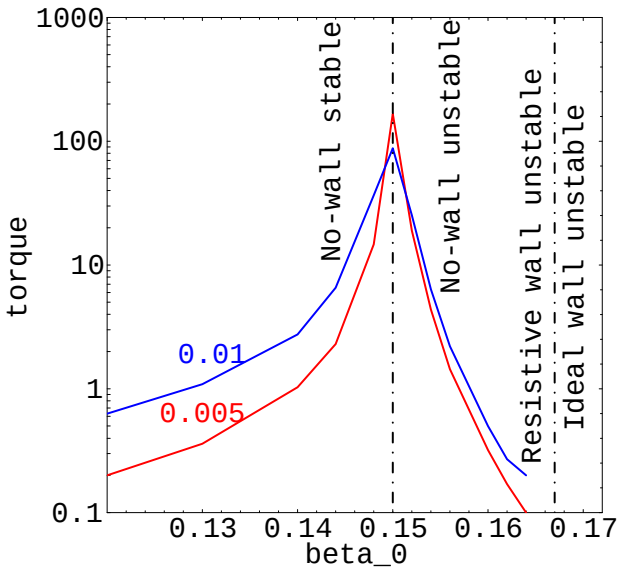

Figure 1: *The torque dependence on plasma beta for ITER, with the rotation frequency as a parameter, for the shear Alfvén resonance.*

$$\mathcal{V}^{-1}\tau_w\frac{\partial}{\partial t}\boldsymbol{d}_{v1} + \mathcal{F}_2^{-1}\delta W_\infty \delta W_b^{-1}\mathcal{F}_1\boldsymbol{d}_{v1}, = -\boldsymbol{J}. \tag{1}$$

Here, $\boldsymbol{d}_{v1}$ is the perturbed normal magnetic field at the wall; $\boldsymbol{J}$ is the jump of the magnetic scalar potential across the error-field layer (which specifies the error-field strength); τ_w is the resistive wall time; δW_∞ and δW_b are the plasma potential energies without and with a wall, respectively; and $\mathcal{F}_{1,2}$ and $\mathcal{V}$ are matrices related to vacuum geometry parameters. From Eq. (1) we can obtain the torque,

$$\tau_\phi^e \;=\; \frac{in\pi}{\mu_0}\boldsymbol{J}^\dagger\mathcal{F}_1^{-1}\delta W_b\delta W_\infty^{-1}\mathcal{F}_2\boldsymbol{J} + cc, \tag{2}$$

and the resistive wall mode growth rate,

$$\tau_w\gamma_{RWM} \;=\; -\frac{1}{2}\mathcal{V}\mathcal{F}_2^{-1}\delta W_\infty\delta W_b^{-1}\mathcal{F}_1 + cc. \tag{3}$$

For the case of a single mode, Eqs. (2) and (3) exhibit the following dependencies:

$$\tau_\phi^e \;\propto\; \frac{\delta W_i(\delta W_{b,r} - \delta W_{\infty,r})}{\delta W_{\infty,r}^2 + \delta W_i^2}|\boldsymbol{J}|^2, \tag{4}$$

$$\tau_w\gamma_{RWM} \;\propto\; \frac{\delta W_{\infty,r}\delta W_{b,r} + |\delta W_i|^2}{\delta W_{b,r}^2 + \delta W_i^2}, \tag{5}$$

where subscripts r and i designate real and imaginary parts, and δW_i is the imaginary part of the plasma energy either with or without a wall. For the shear Alfvén resonance, δW_i is approximately proportional to the toroidal rotation frequency [8]. Note that $\delta W_{b,r} - \delta W_{\infty,r}$, the difference of the resistive wall and no-wall potential energies, depends only on the vacuum energies with and without a wall and therefore is independent of the plasma beta. Equation (4) clearly shows that the torque maximum occurs at the no-wall stability limit ($\delta W_{\infty,r} = 0$), which is different from the resistive wall mode stability limit ($\gamma_{RWM} \propto \delta W_{\infty,r}\delta W_{b,r} + |\delta W_i|^2 = 0$). In particular, the growth rate for the resistive wall mode is negative at the no-wall stability limit, $\gamma_{RWM} \propto -|\delta W_i|^2/(\delta W_{b,r}^2 + \delta W_i^2)$, because the mode is damped due to rotational stabilization.

Applying our new explicit expression for the torque, Eq. (2), we directly computed the torque in ITER for the case of the shear Alfvén resonance, making use of the AEGIS code [10]. Figure 1 shows our result for the torque on the plasma in ITER, as a function of the strength of the error field. One feature of Fig. 1 is that the resonance for static error-field amplification (i.e., the maximum of the static error-field-induced torque) in tokamak plasmas does indeed occur at the no-wall stability limit, instead of at the resistive wall mode stability limit. Another feature of Fig. 1 is that the smaller the rotation, the larger the torque. This indicates that rotation braking is self-enhancing: namely, the error-field-generated torque brakes the rotation, and in return the reduced rotation further enhances the strength of the braking torque.

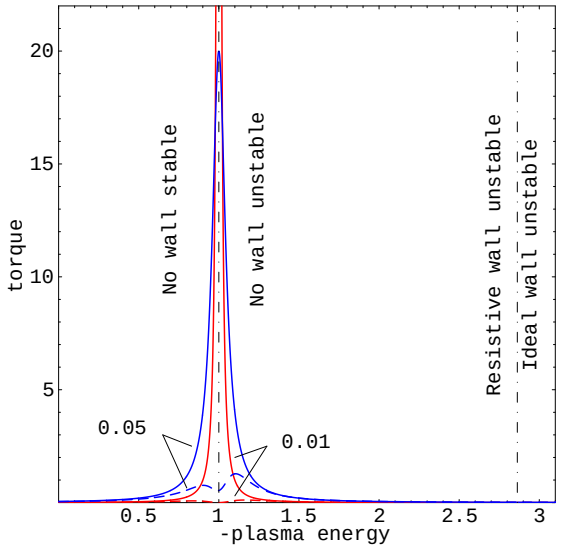

Figure 2: *The torque dependence on plasma beta with (dashed curve) and without (solid curve) a liquid metal wall, with the rotation frequency as a parameter.*

2. Shielding of the Error Field by a Liquid Metal Wall

In order to find ways to ameliorate the effects of the error field, we investigated the presence of a liquid metal wall. Our results show that a flowing liquid metal wall can shield the error field [11], which would otherwise be amplified.

With the liquid metal wall assumed to be thin and located immediately inside the error field structure, we derive the following expression for the torque in the presence of the liquid metal wall:

$$\tau_\phi^e = \frac{in\pi}{\mu_0}\boldsymbol{J}^\dagger\Lambda^\dagger\mathcal{F}_1^{-1}\delta W_b\delta W_\infty^{-1}\mathcal{F}_2\Lambda\boldsymbol{J} + cc., \tag{6}$$

Comparing Eq. (6) with the expression for the torque without a liquid metal wall, Eq. (2), we see that the effect of the liquid metal wall is manifested through the matrix quantity $\Lambda = \mathcal{F}_2^{-1}\delta W_\infty(i\mathcal{V}^{-1}\mathcal{V}_\theta\ \mathcal{M}\mathcal{F}_1^{-1}\delta W_b + \mathcal{F}_2^{-1}\delta W_\infty)^{-1}$, where $\mathcal{V}_\theta$ is the flow speed of the liquid metal. Because the torque without a liquid metal wall is inversely proportional to δW_∞, whereas with a liquid metal wall it is directly proportional to δW_∞ (because the product $\Lambda^\dagger\Lambda$ scales as δW_∞^2), we find that the presence of a liquid metal wall causes a dramatic difference. Indeed, as shown in Fig. 2, in the presence of a liquid metal wall, we find that the torque maximum at the no-wall stability limit ($\delta W_{\infty,r} = 0$) is suppressed and becomes a torque minimum. The self-enhancing synergy in rotation braking is also reversed to

become a negative feedback process so that the smaller the rotation, the weaker the torque peak.

By analogy to the case with a liquid metal wall, we can also demonstrate that a resistive wall is able to play a role in dynamically shielding the effect of the error field, as follows. The error field brakes the rotation. Consequently, the decreasing rotation leads to a time-dependent system, even though the error field itself is static. Then, by drawing a parallel between the $\partial/\partial t$ term in the equation of motion for the resistive wall case and the $\vec{v} \cdot \nabla$ term for the liquid metal wall case, we find that the resistive wall can also provide a dynamical shielding effect on the static error field.

3. Spontaneous Generation of Rotation due to Cyclotron Heating

Also related to rotation, we have examined the experimental observation of spontaneous plasma rotation that is generated by ion or electron cyclotron wave heating in Alcator C-Mod, DIII-D, JET, and Tore Supra, despite the lack of auxiliary mechanical momentum input [12, 13, 14, 15]. Previous explanations for this spontaneous rotation were based either on toroidal torque created by a radial electric field due to orbit shifts of wave-heated energetic particles or on turbulence-induced toroidal stress [16, 17, 18, 19]. Here, we provide an alternative theoretical explanation, in which the cyclotron heating can be a direct drive for tokamak plasma rotation [20]. Even with the cyclotron heating applied symmetrically, without a preferred toroidal direction, we find that, when finite Larmor radius effects and the magnetic field inhomogeneity are taken into account, the toroidal momentum input due to cyclotron wave heating is unbalanced in the toroidal direction. The cyclotron heating accelerates a population of trapped energetic particles through their toroidal precessional drift. The toroidal momentum input is then conveyed to the core plasma through collisions.

We use quasilinear theory [21, 22, 23] to calculate the toroidal rotation drive due to cyclotron wave heating. The plasma equilibrium distribution function is a function of three independent adiabatic invariants: the magnetic momentum $M = (m^2/e)\mu$, the canonical angular momentum $P = m\dot{\zeta}R^2 - e\psi$, and the longitudinal invariant $J_\theta = (e/2\pi)\int d\beta\alpha$, where m and e are the mass and charge, a dot denotes a time derivative, and $\mu = v_\perp^2/2B$, with $v_\perp$ the perpendicular particle velocity. These three invariants can be used to construct the action vector $\boldsymbol{J} = (M, P, J_\theta)$. The corresponding angle vector is $\boldsymbol{\theta} = (\theta_g, \varphi, \theta)$, where θ_g is the gyro phase, and where for trapped particles $\varphi = \zeta - q\beta$, and $\theta = (\pi/2)F(\xi,\kappa)/K(\kappa)$ [22]. Here, $\kappa = \sin(\theta_t/2)$ with θ_t the turning point, K is the complete elliptic integral of the first kind, and F is the normal elliptic integral of the first kind, with ξ defined by $\kappa\sin(\xi) = \sin\beta/2$. Related to the three angular motions $\boldsymbol{\theta}$, there is the frequency vector $\boldsymbol{\omega} = (\omega_c, \omega_\theta, \omega_\varphi)$, with three components describing respectively the gyro frequency ω_c, the bounce frequency ω_θ, and the toroidal precessional frequency ω_φ [25]:

$$\omega_c = \frac{eB}{m},\ \omega_\theta = \frac{\pi v_\perp (r/R)^{1/2}}{2^{3/2} qRK(\kappa)},\ \omega_\varphi = \frac{v_\perp^2 q}{2Rr\omega_c} D(\kappa),$$

where

$$D(\kappa) = 4s\frac{E(\kappa) + (\kappa^2 - 1)K(\kappa)}{K(\kappa)} + \frac{2E(\kappa) - K(\kappa)}{K(\kappa)}, \tag{7}$$

$E(\kappa)$ is the complete elliptic integral of the second kind, and s is the magnetic shear. The first term on the right-hand side of Eq. (7) results from the effect of finite banana width.

In action-angle variables, the linear and quasilinear equations for the slowly varying equilibrium distribution function F_0 and the linear perturbed distribution function δf are as

follows [21, 22]:

$$\frac{\partial \delta f}{\partial t} + \boldsymbol{\omega} \cdot \frac{\partial \delta f}{\partial \boldsymbol{\theta}} = -\delta \dot{\boldsymbol{J}} \cdot \frac{\partial F_0}{\partial \boldsymbol{J}}, \tag{8}$$

$$\frac{\partial \langle F_0 \rangle}{\partial t}(\boldsymbol{J}; t) = -\frac{\partial}{\partial \boldsymbol{J}} \cdot \left\langle \delta \dot{\boldsymbol{J}} \delta f \right\rangle, \tag{9}$$

where $\langle \cdots \rangle$ denotes an average over all components of $\boldsymbol{\theta}$. The perturbed action vector $\delta \boldsymbol{J}$ can be determined by $\delta \dot{\boldsymbol{J}} = -\partial \delta H / \partial \boldsymbol{\theta}$, where δH is the perturbed Hamiltonian. Solving Eqs. (8) and (9) yields [24]

$$\begin{aligned}
\delta f_l &= \frac{\pi e^2}{l \omega_c m^2 c |k_\parallel|} v_\perp \left(\delta E^+ J_{l-1} + \delta E^- J_{l+1} \right) \\
&\quad \times \delta \left(v_\parallel - \frac{\omega - k_\varphi \omega_\varphi - l\omega_c}{k_\parallel} \right) \frac{\partial F_0}{\partial \mu} \exp\{i \boldsymbol{k} \cdot \boldsymbol{r}\}, \\
\frac{\partial \langle F_0 \rangle}{\partial t} &= \frac{\pi e^2}{2 m^2 |k_\parallel|} \sum_{l=-\infty}^{+\infty} \frac{1}{l^2 v_\perp} \frac{\partial}{\partial v_\perp} v_\perp \left| \delta E^+ J_{l-1} + \delta E^- J_{l+1} \right|^2 \\
&\quad \times \delta \left(v_\parallel - \frac{\omega - k_\varphi \omega_\varphi - l\omega_c}{k_\parallel} \right) \frac{\partial \langle F_0 \rangle}{\partial v_\perp},
\end{aligned} \tag{10}$$

where δf_l are the Fourier components of δf with respect to the gyro phase, $k_\parallel$ is the parallel wave number, and k_φ is the toroidal wave number. Using Eq. (10), we calculate the toroidal momentum input rate from the cyclotron heating:

$$T_\zeta = \int d^3 v m R \omega_\varphi \frac{\partial \langle F_0 \rangle}{\partial t} = \frac{q}{2 r \omega_c} D(\kappa) P_w, \tag{11}$$

where q is the safety factor and P_w is the energy absorption rate per volume from the cyclotron waves [23],

$$P_w = \frac{\pi e^2}{4 m |k_\parallel|} \left| \delta E_x \pm i \mathrm{sgn}(\omega) \delta E_y \right|^2 n_{res}, \tag{12}$$

with upper and lower sign for ions and electrons, respectively. n_{res} is the number of resonant particles

$$n_{res} = \int d^3 v \delta \left(v_\parallel - \frac{\omega - k_\varphi \omega_\varphi - l\omega_c}{k_\parallel} \right) \langle F_0 \rangle .$$

We can now use the expression for the toroidal momentum input rate, Eq. (11), to interpret various observed features of the spontaneous rotation due to cyclotron heating. For the sake of brevity, we focus on the case of ion cyclotron radio-frequency heating, with a few comments about the case of electron cyclotron heating.

Scaling with stored energy and current: Since the safety factor q is inversely proportional to the plasma current I_p, we see from Eq. (11) that $T \propto P_w / I_p$, i.e., the toroidal rotation scales as the energy absorbed from the cyclotron heating, normalized to the plasma current. This scaling agrees with the experimental observations [26].

Direction of rotation for on-axis heating: For on-axis RF heating, the location of the resonant heating surface is $r_{res} = 0$ (see Fig. 3). For this case, the turning points are $\theta_t = \pm \pi/2$ for all resonant trapped particles, and consequently the quantity $D(\kappa)$ is

positive and independent of minor radius r. Hence the sign of the toroidal rotation is determined by the sign of the resonant particle charge and the "sign" of the safety factor. We conclude that the direction of rotation is co-current for ion cyclotron resonant heating ($\omega_c > 0$), but counter-current for electron cyclotron heating ($\omega_c < 0$). Furthermore, since the safety factor is inversely proportional to the current, we find that the direction of the rotation reverses when the plasma current is reversed.

Direction of rotation for off-axis heating: Consider off-axis heating with the resonance on the high-field side ($r_{res} < 0$). For this case, as shown in Fig. 3, the turning points at the resonance heating surface are a function of the radial location r of the trapped particles. Resonant trapped particles located at small radii have large turning points, and consequently their toroidal precessional velocities can be drift-reversed, in contrast to the non-drift-reversed trapped particles located at larger radii. This feature is consistent with internal transport barrier discharges with off-axis cyclotron heating, in which the plasma rotation is observed to be counter-current near the axis, but co-current at larger radii [27].

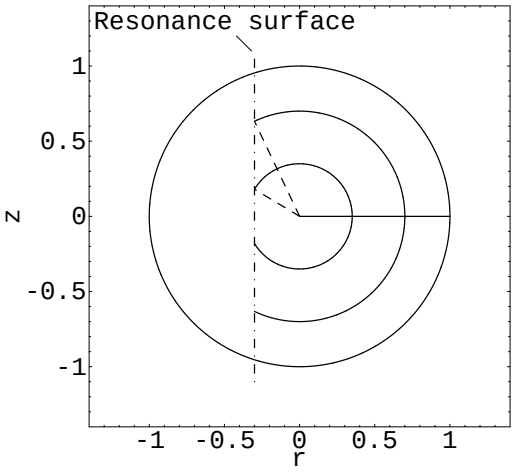

Figure 3: *Tokamak plasma cross section showing the dependence of the turning point θ_t on the minor radius r. The cyclotron wave resonance surface is the dot - dashed line.*

Radially inverted rotation profile: Experimental observations show that the rotation has a radially inverted profile, being stronger at large radii and weaker toward the center, and that after an L-to-H transition the rotation and stored energy in the core rapidly increase. This has been interpreted to mean that rotation is transported from the outer region to the center. Our explanation provides a different picture. The function $D(\kappa)$ in Eq. (11) depends on the magnetic shear, through the banana width effect. For a monotonically increasing q profile, the magnitude of D increases with r and could thus contribute to a radially increasing rotation profile. Also, following a L-H transition, the central plasma density becomes peaked, which can lead to enhanced absorption of wave energy in the center, so that — according to Eq. (11) — the core rotation is increased.

Magnitude of rotation: We already pointed out that our theory gives the correct scaling of the rotation velocity with the absorbed energy and the plasma current. Now we wish to show that the predicted magnitude of the rotation agrees with experiment. In Ref. [28], the C-Mod experimental data were fitted with the line $v_\zeta[\mathrm{m/s}] \approx 10^6\ W[\mathrm{J}]/I_p[\mathrm{A}]$. We note, however, that the rotation velocity in this fit corresponds to the maximum value. A detailed examination of the experimental time histories of the stored energy and central toroidal rotation velocity, as shown in Fig. 4, shows that the energy absorbed from the ICRF heating saturates early, while the rotation speed continues to increase. This indicates that the energy and momentum are governed by different transport mechanisms, with the energy confinement time shorter than the momentum confinement time in these H-mode plasmas. The rotation velocity rises until the ICRF power is reduced. No rotation braking from the error field is evident, since the plasma beta is lower than the no-wall stability limit. When the ICRF is turned off, instabilities (indicated by the D_α signal) cause the rotation to be braked. Although the stored energy and momentum time histories differ, we can use the short time period Δt (between the two red vertical lines in Fig. 4) before the energy saturates to estimate the stored energy gain. During this short period, the D_α emission remains low and the energy loss due to transport is relatively

small. We see that both the stored energy and also the rotation speed increase linearly within this time period. The stored energy W increases from 50 kJ to 100 kJ due to the ICRF heating, while the rotation velocity goes from zero to $(1-2)10^4$m/s, giving the ratio $v_\zeta[\mathrm{m/s}]/W[\mathrm{J}] = 0.2-0.4$. The value of v_ζ used here is about 20% of the maximum rotation speed. Now we theoretically estimate the rotation speed from Eq. (11). The stored energy gain is $\delta W = P_w\ \Delta t\ V_0$, with $V_0 = 2\pi^2 R a^2$ the plasma volume; for C-Mod the minor and major radii are $R = 0.67$ m and $a = 0.21$ m. The gain in rotation speed is $\Delta v_\zeta = T\Delta t/n_0 m_\rho$, with n_0 the density and m_ρ the ion mass. Thus, from Eq. (11), we obtain

$$\Delta v_\zeta[\mathrm{m/s}]/\Delta W[\mathrm{J}] = 0.1 f_v \left\langle q \right\rangle_v / A \rightarrow 0.2-0.5, \tag{13}$$

where $f_v \sim 2-3$ is the ratio of the central rotation speed to the volume-averaged rotation speed, $\langle q\rangle_v \sim 2-3$ is the volume-averaged value of q, and $A = 2$ is the ratio of the ion mass to the proton mass. The value in Eq. (13) is thus in reasonable agreement with the experimental data in Fig. 4. Note that the rotation velocity estimated here represents the sustainable bulk plasma rotation; the trapped particle rotation velocity can be larger until the rotation speeds of the minority particles and the bulk plasma are equilibrated through collisions. Finally, if we estimate the plasma current as $I_p = 2\pi a^2 B/\mu_0 R q(a) = 1MA$ for C-Mod parameters, we obtain from Eq. (13) the ratio $v_\zeta[\mathrm{m/s}]/(W[\mathrm{J}]/I_p[\mathrm{A}]) \approx 3\times 10^5$, which is consistent with the experimental fit in Ref. [28] mentioned above.

Acknowledgment: This research was supported by the Office of Fusion Energy Science of the U.S. Department of Energy under Grant DE-FG02-04ER54742.

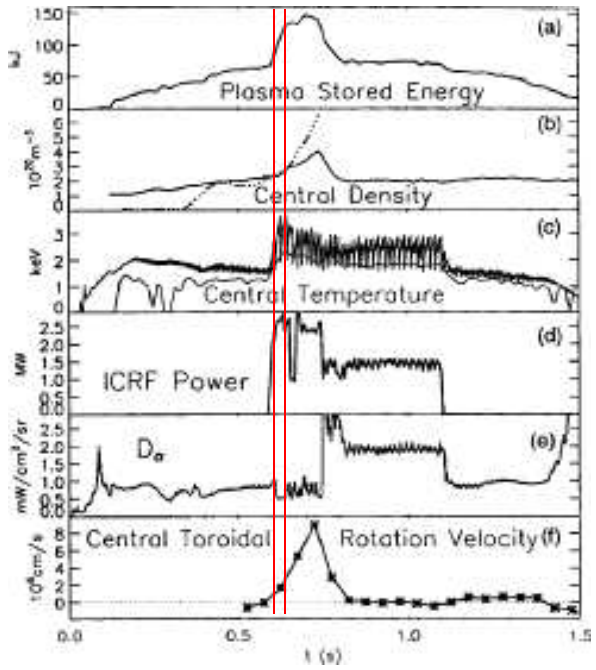

Figure 4: *Time histories of stored energy, central density and temperature, ICRF power, D_α emission, and central toroidal rotation velocity for a 5.4 T deuterium H mode discharge in C-Mod. This is Fig. 6 in Ref. [12] with two vertical lines added.*

References

[1] GAROFALO, A. M., *et al.*, Phys. Rev. Lett. **82** (1999) 3811.

[2] BOOZER, A. H., Phys. Rev. Lett. **86** (2001) 5059.

[3] GAROFALO, A. M., *et al.*, Phys. Plasmas **9** (2002) 1997.

[4] GIMBLETT, C. G., HASTIE, R. J., Phys. Plasmas **11** (2004) 1019.

[5] BOOZER, A. H., Phys. Plasmas **10** (2003) 1458.

[6] GAROFALO, A. M., JENSEN, T. H., STRAIT, E. J., Phys. Plasmas **10** (2003) 4776.

[7] ZHENG, L.-J., KOTSCHENREUTHER, M. T., to be published in Phys. Rev. Lett. (2006).

[8] ZHENG, L.-J., KOTSCHENREUTHER, M. T., CHU, M. S., Phys. Rev. Lett **95** (2005) 255003.

[9] FREIDBERG, J. P., Ideal Magnetohydrodynamics (Clarendon, Oxford, 1987).

[10] ZHENG, L.-J., KOTSCHENREUTHER, M. T., J. Comput. Phys. **221** (2006) 748.

[11] ZHENG, L.-J., KOTSCHENREUTHER, M. T., WAELBROECK, F. L., Nucl. Fusion **46** (2006) L9.

[12] RICE, J. E.,GREENWALD, M., HUTCHINSON, I. H., *et al.*, Nucl. Fusion **38** (1998) 75.

[13] ERIKSSON, L. G., RIGHI, E., ZASTROW, K. D., Plasma Phys. Controlled Fusion **39** (1997) 27.

[14] DEGRASSIE, J. S., BURRELL, K. H., BAYLOR, L. R., HOULBERG, W., LOHR, J., Phys. Plasmas **11** (2004) 4323.

[15] HOANG, G. T.,MONIER-GARBET, P., ANIEL, T., *et al.*, Nucl. Fusion **40** (1999) 913.

[16] CHAN, V. S., CHIU, S. C., OMELCHENKO, Y. A., Phys. Plasma **9** (2002) 501.

[17] ERIKSSON, L.-G. *et al.* Phys. Rev. Lett. **92** (2004) 235001

[18] SHAING, K. C., Phys. Rev. Lett. **86** (2001) 640.

[19] COPPI, B., Nucl. Fusion **42** (2002) 1.

[20] ZHENG L.-J., VAN DAM J. W., and KOTSCHENREUTHER M. to be submitted to Phys. Rev. Lett.

[21] KAUFMAN, A. N., Phys. Fluids **15** (1972) 1063.

[22] HAZELTINE, R. D., MAHAJAN, S. M., HITCHCOCK, D. A., Phys. Fluids **24** (1981) 1164.

[23] STIX, T. H., Waves in plasmas (American Institute of Physics, New York, 1992).

[24] OSIPENKO, M. V. and SHURYGIN R. V. Sov. J. Plasma Phys. **16** (1990) 824.

[25] WHITE, R. B., The theory of toroidal confined plasmas (American Institute of Physics, New York, 1992).

[26] RICE, J. E., LEE, W. D., MARMAR, E. S., *et al.*, Phys. of Plasmas **11** (2004) 2427.

[27] RICE, J. E., LEE, W. D., MARMAR, E. S., *et al.*, Nucl. Fusion **44** (2004) 379.

[28] RICE, J. E. *et al.*, Nucl. Fusion **41** (2001) 277.